Monovalent and Divalent Cations at the α-Al_2O_3(0001)/Water Interface: How Cation Identity Affects Interfacial Ordering and Vibrational Dynamics

Stefan M. Piontek[1], Aashish Tuladhar[1, 2], Tim Marshall[1], and Eric Borguet[,1]*

1 Department of Chemistry, Temple University, 1901 N. 13th St., Philadelphia. PA 19122, USA

2 Physical Sciences Division, Physical and Computational Sciences Directorate, Pacific Northwest National Laboratory, Richland, WA 99352, USA

AUTHOR INFORMATION

Corresponding Author

eborguet@temple.edu

SUPPORTING INFORMATION

Comparison of Monovalent and Divalent Spectral Profiles at pH 4 Conditions

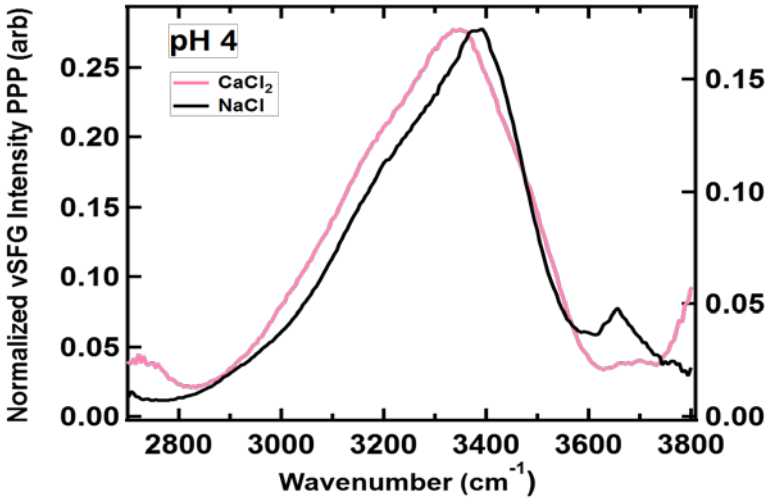

Figure S1: vSFG spectra taken using PPP geometry of 0.1 M NaCl and $CaCl_2$ salts at a positively (pH 4) charged α–$Al_2O_3(0001)/H_2O$ interface. VSFG spectra have been normalized with respect to the shape of the infrared pulse profile and Fresnel factors. Spectra have been normalized to compare spectra shape.

Fitting of Steady State vSFG Data

The vSFG intensity (Equation 1) is proportional to the intensities of incident IR and visible beams, and the second-order susceptibility tensor $\left(\chi^{(2)}\right)$ which contains all the molecular response information for the system (Equation 1) [3]. The $\chi^{(2)}$ can be factored into two terms, a nonresonant term, $\chi_{NR}^{(2)}$ which accounts for the instantaneous electronic response of the system, and a vibrationally resonant $\chi_R^{(2)}$ term which is summed over the available oscillators within the infrared bandwidth. In this model each vibrationally resonant mode is described by a Lorentzian line shape,[4] where ω_{IR} is the frequency of the driving infrared pulse, φ_{NR} is the phase associated with the nonresonant contribution, and A_v, ω_v, and Γ_v are the amplitude, central frequency, and damping coefficient of the v^{th} vibrational mode, respectively. While the spectral range that was fit to was kept mostly constant, clearly resonant features were given higher priority. For CsCl pH 10 steady state vSFG spectra (**Figure S2**), the ~2800-2950 cm^{-1} spectral range was assigned mainly to the nonresonant background, and thus was not considered valuable in gaining insight into the orientation of resonant species in the interfacial region.

$$I_{SFG} \propto \left|\chi^{(2)}\right|^2 I_{Vis} I_{IR} = \left|\chi_{NR}^{(2)} + \sum_v \chi_R^{(2)}\right|^2 I_{Vis} I_{IR} \qquad (S1)$$

$$= \left|\chi_{NR}^{(2)} e^{i\varphi_{NR}} + \sum_v \frac{A_v}{\omega_{IR} - \omega_v + i\Gamma_v}\right|^2 I_{Vis} I_{IR}$$

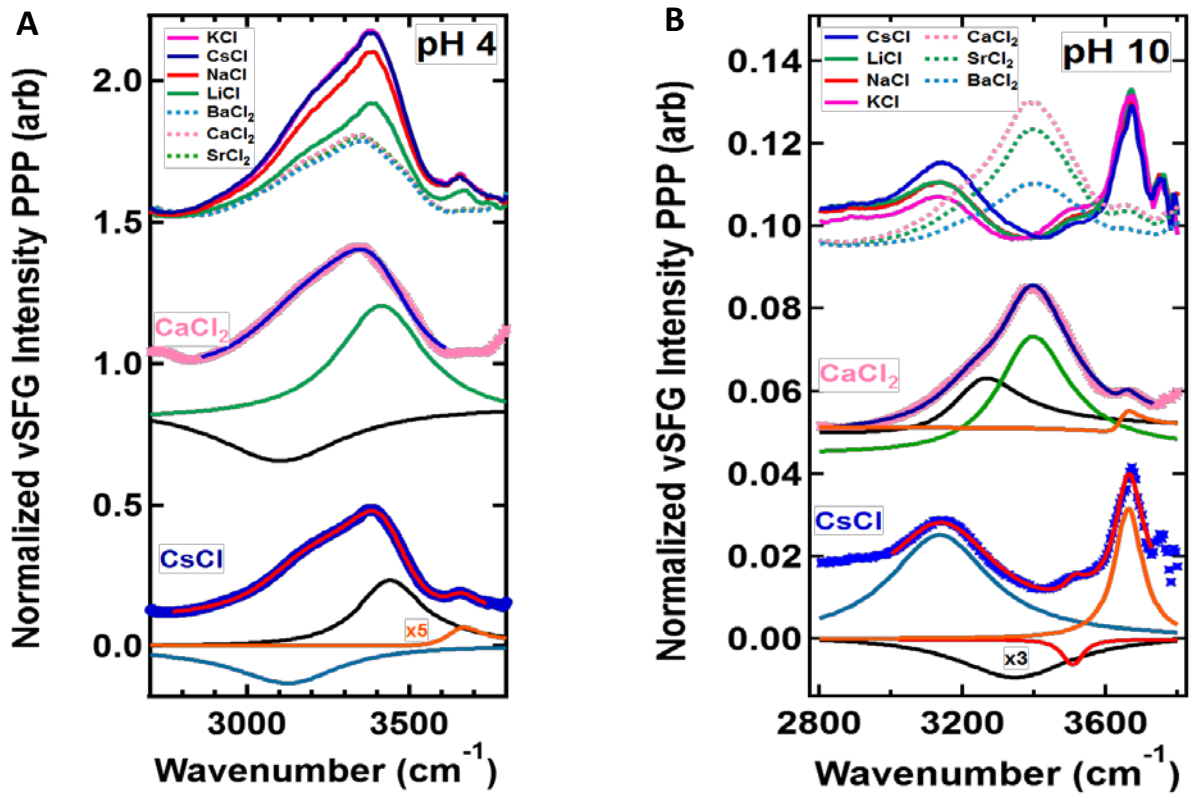

Figure S2: PPP vSFG spectra of the α–Al_2O_3(0001) /water interface at pH 4 A) and pH 10 B) with 0.1 M electrolyte solutions. Monovalent cation solutions are displayed with solid lines and divalent cation solutions with dashed lines. The effects of CsCl and $CaCl_2$ at A) pH 4 and B) pH 10. All spectra were fit with **Equation S1.** The solid lines overlaid on the data display the total fit to **Equation S1.** Fit parameters for selected pH 4 and pH 10 spectra can be found in **Table S1** and **Table S2**, respectively.

	pH 4 H_2O CsCl $Chi^2 = 2.8 \times 10^{-4}$			**pH 4 H_2O $CaCl_2$** $Chi^2 = 1.6 \times 10^{-4}$	
Species	**Strongly H-Bonded Species**	**Weakly H-Bonded Species**	**Free OH (Out of Plane Aluminol)**	**Strongly H-Bonded Species**	**Weakly H-Bonded Species**
ω_v (cm^{-1})	3142	3430	3652	3101	3414
ψ (rad)	0 assigned to χ_{NR}			0 assigned to χ_{NR}	
A_v (arb)	-72	60	7.2	-47	47
Γ_v (cm^{-1})	200	123	68	240	165
X_{NR}	0.030			0.001	

Table S1: Fit parameters for Lorentzian fits (**Equation 1**) for pH 4 α-Al_2O_3(0001) /H_2O + 0.1 M electrolyte spectra taken in PPP geometry (**Figure S2**). The highly blue shifted species at ~3650 cm^{-1} is present for pH 4 CsCl but not

for CaCl2. Both spectra require one weakly and strongly hydrogen bonded species with opposite amplitudes. The phase associated with the nonresonant contribution to the spectra is held at 0.

	pH 10 H_2O CsCl $Chi^2 = 8.0 \times 10^{-5}$				pH 10 H_2O $CaCl_2$ $Chi^2 = 4.3 \times 10^{-5}$		
Species	**Strongly H-Bonded Species**	**Weakly H-Bonded Species 1**	**Weakly H-Bonded Species 2**	**Free OH (Out of Plane Aluminol)**	**Strongly H-Bonded Species**	**Weakly H-Bonded Species**	**Free OH (Out of Plane Aluminol)**
ω_v (cm^{-1})	3135	3350	3508	3663	3241	3389	3650
ψ (rad)	0 assigned to χ_{NR}				0 assigned to χ_{NR}		
A_v (arb)	26	-11	-3	8	5.5	20	0.50
Γ_v (cm^{-1})	170	193	34	46	114	121	29
X_{NR}	0.001				0.012		

Table S2: Fit parameters for Lorentzian fits (**Equation S1**) for pH 10 α–Al_2O_3(0001) /H_2O + 0.1 M electrolyte spectra taken in PPP geometry (**Figure S1**). Interference between the strongly and weakly hydrogen bonded water species is manifested in opposite amplitude oscillators. There is also a large enhancement of the free OH species at 3663 cm^{-1} in the CsCl spectrum not present in the $CaCl_2$ spectrum. No interference is observed for interfacial oscillators in the case of pH 10 $CaCl_2$, indicating all species are in phase with another.

Four Level Model Used to Fit Time Resolved vSFG Dynamics

Due to the double-exponential kinetics displayed by interfacial O-H stretches recovering to a hot ground state seen in this work and previously by others[1, 5-8], a four-level system[1, 5-9] (**Figure S3**) was used to fit the TR-vSFG response.

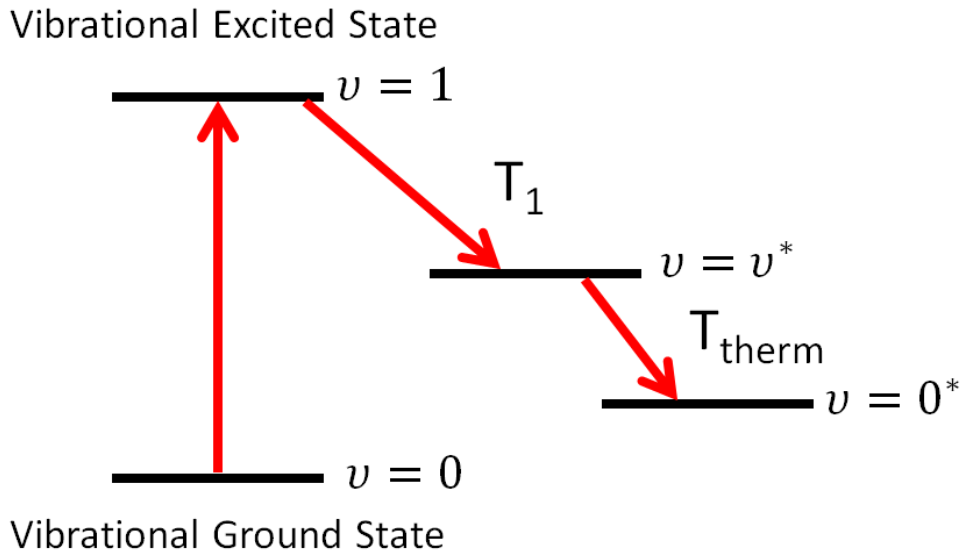

Figure S3: Schematic the four level model used to fit time resolved vSFG spectra of electrolyte solutions at the α-Al_2O_3(0001)/H_2O Interface. The pump infrared pulse achieves the initial transition from ν = 0 to ν = 1 , while recovery to a hot intermediate state indicative of the excited O-H stretch lifetime is monitored by the probe infrared pulse.

The transfer of population between energy levels are described by four coupled differential equations:

$$\frac{dN_0}{dt} = -\sigma I_{pu}(t)(N_0 - N_1) \quad \text{(S2)}$$

$$\frac{dN_1}{dt} = \sigma I_{pu}(t)(N_0 - N_1) - \frac{N_1}{T_1} \quad \text{(S3)}$$

$$\frac{dN_2}{dt} = \frac{N_1}{T_1} - \frac{N_2}{T_{therm}} \quad \text{(S4)}$$

$$\frac{dN_3}{dt} = \frac{N_2}{T_{therm}} \quad \text{(S5)}$$

Where the $v = 0$, $v = 1$, v^*, and $v^* = 0$ energy levels have populations denoted by N_0, N_1, N_2, and N_3 respectively. The infrared cross section of the vibrational ground state ($v = 0$) is denoted by σ. The Gaussian temporal profile of the pump pulse is $I_{pu}(t)$ and the pump pulse has a width of τ at half the maximum intensity which is used to describe the instrument response function. The time constants assigned to the vibrational relaxation and thermalization process are given by T_1 and T_{therm} , respectively[7].

The solution to equations S2-S5 describes the population transfer between N_0, N_1, N_2, and N_3 as a function of time (t). Subsequent substitution of the solution into the equation for the vSFG response and convolution with a Gaussian instrument response function (IRF trace) gives:

$$I_{SFG} = IRF(t) * [N_0(t) - N_1(t) + C_2N_2(t) + C_3N_3(t)]^2 + I_F \quad \text{(S5)}$$

Here C_2 and C_3 are constants that are related to the optical nonlinear susceptibilities of the intermediate and hot ground state, and I_F is the magnitude of the vSFG response at t = 3 picoseconds[7]. Nine parameters are used in the fit as can be seen in **Table S3**. N_0 is held at 1 since the magnitude of the vSFG response is normalized to 1 before the arrival of the pump pulse. On the time scale of our TR-vSFG experiments (3 ps scan) thermalization is not observed, and T_{therm} was fixed at 600 femtoseconds. The t = 0 position is given at the maximum intensity of the third order cross-correlation ($\chi^{(3)}$) between the infrared pump, infrared probe, and visible beam. The time at which the maximum bleach of the vSFG response is achieved can vary slightly from the TR-vSFG of the nonresonant gold coated prism and a small offset is added to the x axis (time) to account for this. In most cases it is on the order of +/- 50 fs.

Limitations of the Four Level Model

While the four level model assumes that a single vibrational mode is being pumped and probed, multiple O-H stretch modes lie within the probe pulse which has ~ 250 cm^{-1} of FWHM

bandwidth centered at ~3150 cm^{-1}. Our past spectrally resolved TR-vSFG[5] data suggests that the kinetics of vibrational relaxation for both species are not spectrally homogeneous. The bandwidth of our pumping and probing window does not cover the entire O-H stretch region, which means that fast spectral diffusion can lead to blue shifted O-H stretch species that have a natural frequency outside the probe window. This can lead to an extracted T_1 lifetime that is faster than the true vibrational lifetime of the mode. Due to both of these concerns we are measuring an apparent lifetime and not necessarily the true vibrational lifetime of a single vibrational mode. The model and extracted T_1 lifetimes do provide useful information about the ability of interfacial water to redistribute vibrational energy in the presence of mono and divalent salts.

Fitting Parameters for Time Resolved vSFG Data In Figure 3

	0.1 M NaCl in H_2O	
	pH 4	**pH 10**
N_0	1	1
t_o	-0.038 ± 0.065	-0.04 ± 0.10
σ	2.74 ± 0.38	1.52 ± 0.37
τ	0.075 ± 0	0.075 ± 0
C_2	0.70 ± 0.10	1.35 ± 0.2
C_3	0.61 ± 0.059	1.33 ± 0.10
Os	-0.99 ± 0.007	-0.988 ± 0.005
T_1	0.13 ± 0.012	0.117 ± 0.016
T_{Therm}	0.6	0.6

Table S3: Fit parameters for time resolved vSFG data of pH 4 (**Figure 3)** and pH 10 0.1 M NaCl in H_2O solutions taken at the α-Al_2O_3(0001)/H_2O interface using PPP experimental geometry. T_{Therm} and N_0 were the only fixed parameters.

	0.1 M $BaCl_2$ in H_2O	
	pH 4	**pH 10**
N_0	1	1
t_o	-0.041 ± 0.033	-0.047 ± 0.053
σ	4.55 ± 0.31	3.64 ± 0.31
τ	0.075 ± 0	0.075 ± 0
C_2	0.85 ± 0.054	0.64 ± 0.042
C_3	0.75 ± 0.025	0.61 ± 0.031
Os	-0.99 ± 0.0064	-0.99 ± 0.004
T_1	0.12 ± 0.006	0.11 ± 0.008
T_{Therm}	0.6	0.6

Table S4: Fit parameters for time resolved vSFG data of pH 4 (**Figure 3)** and pH 10 0.1 M $BaCl_2$ in H_2O solutions taken at the α-Al_2O_3(0001)/H_2O interface using PPP experimental geometry. Again, T_{Therm} and N_0 were the only fixed parameters.

Time Resolved vSFG Spectra of Other Mono and Divalent Cations

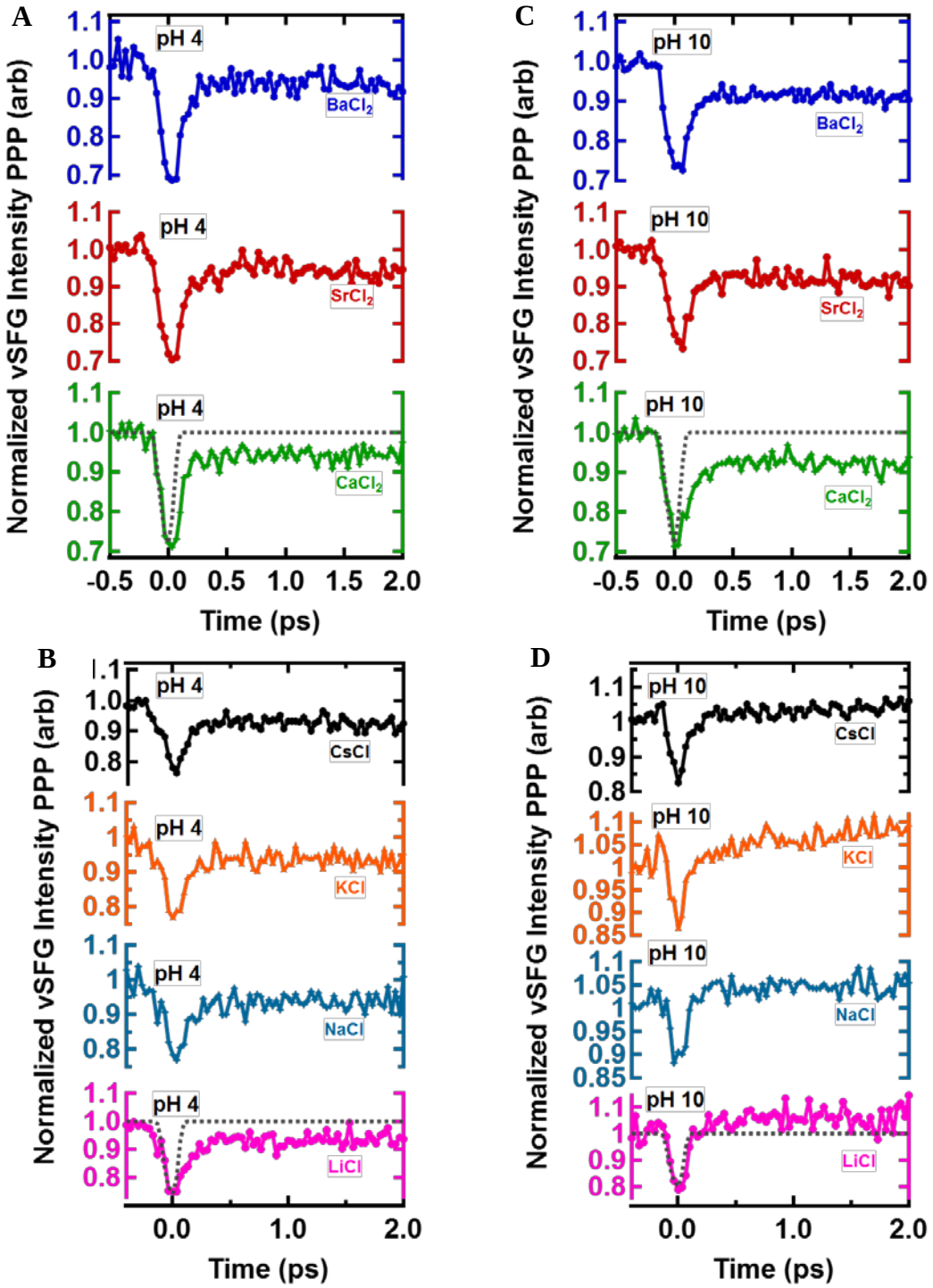

Figure S4: Time Resolved vSFG spectra of 0.1 M monovalent and 0.1 M divalent cations at pH 4 A-B) and pH 10 C-D) recorded in PPP geometry. The third-order cross-correlation between IR pump, IR probe, and visible is shown by the black dashed line and has a FWHM of ~105 fs, suggesting IR pulse durations of ~75 fs. The displayed traces are the average of two scans.

Integration Times for Steady State and Time Resolved vSFG Data

A variety of integration times were used, depending on the signal levels, as the ion identity and bulk pH were varied. Steady state SFG experiments with monovalent cations typically required ~30-60 seconds integration times to acquire high quality spectra. Time resolved measurement integration times were more sensitive to the pH, and ranged from 1-20 seconds per 33 fs time step. This corresponds to 121-2420 sec per scan. The average of 2 scans is presented in all TR-vSFG data shown in this work.

Elements of Nonlinear Susceptibility Probed Using PPP Experimental Geometry

By calculating the Fresnel factors at our experimental angles of incidence, we can comment on which elements of the total nonlinear susceptibility associated with PPP geometry see the largest enhancement from local field effects. The calculation of the Fresnel factors associated with the individual elements of the PPP nonlinear susceptibility at a fixed IR internal angle of 60 degrees as the visible is scanned shows the largest Fresnel factor enhancement for the χ_{zzz} term is found near the critical angle. While the magnitude the Fresnel coefficients associated with of the $\chi_{xxz,}$ $\chi_{xzx,}$ and $\chi_{zxx,}$ are not 0, the Fresnel coefficient for the χ_{zzz} term is much larger, allowing us to primarily sample the χ_{zzz} term. Our experimental geometry is chosen to ensure we are near total internal reflection, with our internal visible and IR angle chosen as 54^o and 60^o respectively.

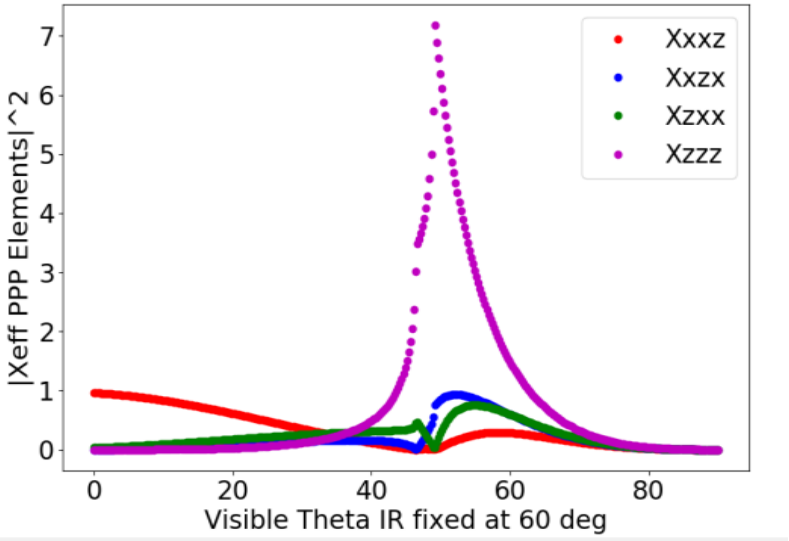

Figure S5: Plotted Fresnel coefficients associated with individual elements of the total nonlinear susceptibility associated with PPP experimental geometry. The local field enhancement associated with the χ_{zzz} element of the total PPP nonlinear susceptibility is the largest in total internal reflection (TIR) geometry.

References

1. Tuladhar, A.; Piontek, S. M.; Borguet, E., Insights on Interfacial Structure, Dynamics, and Proton Transfer from Ultrafast Vibrational Sum Frequency Generation Spectroscopy of the Alumina(0001)/Water Interface. *Journal of Physical Chemistry C* **2017,** *121* (9), 5168-5177, 10.1021/acs.jpcc.7b00499.
2. Tuladhar, A.; Dewan, S.; Kubicki, J. D.; Borguet, E., Spectroscopy and Ultrafast Vibrational Dynamics of Strongly Hydrogen Bonded OH Species at the alpha-Al_2O_3(1120)/H_2O Interface *Journal of Physical Chemistry C* **2016,** *120* (29), 16153-16161, 10.1021/acs.jpcc.5b12486.
3. Wang, H. F.; Gan, W.; Lu, R.; Rao, Y.; Wu, B. H., Quantitative spectral and orientational analysis in surface sum frequency generation vibrational spectroscopy (SFG-VS). *International Reviews in Physical Chemistry* **2005,** *24* (2), 191-256, 10.1080/01442350500225894.
4. Wang, H. F.; Velarde, L.; Gan, W.; Fu, L., Quantitative Sum-Frequency Generation Vibrational Spectroscopy of Molecular Surfaces and Interfaces: Lineshape, Polarization, and Orientation. In *Annual Review of Physical Chemistry, Vol 66*, Johnson, M. A.; Martinez, T. J., Eds. 2015; Vol. 66, pp 189-216.
5. Tuladhar, A.; Piontek, S. M.; Frazer, L.; Borguet, E., Effect of Halide Anions on the Structure and Dynamics of Water Next to an Alumina (0001) Surface. *Journal of Physical Chemistry C* **2018,** *122* (24), 12819-12830, 10.1021/acs.jpcc.8b03004.
6. McGuire, J. A.; Shen, Y. R., Ultrafast Vibrational Dynamics at Water Interfaces. *Science* **2006,** *313* (5795), 1945-1948, 10.1126/science.1131536.
7. Eftekhari-Bafrooei, A.; Borguet, E., Effect of Electric Fields on the Ultrafast Vibrational Relaxation of Water at a Charged Solid-Liquid Interface as Probed by Vibrational Sum Frequency Generation. *Journal of Physical Chemistry Letters* **2011,** *2* (12), 1353-1358, 10.1021/jz200194e.
8. Eftekhari-Bafrooei, A.; Borguet, E., Effect of Surface Charge on the Vibrational Dynamics of Interfacial Water. *Journal of the American Chemical Society* **2009,** *131* (34), 12034-+, 10.1021/ja903340e.
9. Smits, M.; Ghosh, A.; Bredenbeck, J.; Yamamoto, S.; Muller, M.; Bonn, M., Ultrafast Energy Flow in Model Biological Membranes. *New J. Phys.* **2007,** *9*, 20, 10.1088/1367-2630/9/10/390.